Journal of GeoSpace Science

ISSN-xxx-xxx
Open Access Biannual Research Journal publish by Institute of Space and Planetary Astrophysics

Journal home page: http://www.jogss.org/

SAR Image Reconstruction Algorithm Based on 2-D Sparse Decomposition and L_0 Norm Optimization

Andon Lazarov and Dimitar Minchev

Burgas Free University

ARTICLE INFO

Article history:
Received 28 August 2015
Received in revised form 8 September 2015
Accepted 12 September 2015
Available online 24 September 2015

Keywords: *synthetic aperture radar, compressed sensing, l_0 norm optimization, sparse decomposition*

ABSTRACT

Synthetic Aperture Radar (SAR) image reconstruction algorithm based on sparse decomposition and l_0 norm minimization is considered. A linear frequency modulation (LFM) signal reflected from the scene, relief of the earth surface, is presented as a matrix multiplication of three matrices: azimuth Inverse Discrete Fourier Transform (IDFT) matrix, image matrix and range IDFT matrix. Image reconstruction procedure based on l_0 norm optimization is applied over reduced number of measurements defined by randomly generated azimuth and range sensing matrix. The geometry of the scene is described by standard "peaks" function. Results of numerical experiments are provided to prove the correctness of the algorithm.

To Cite This Article: Andon Lazarov; Dimitar Minchev., SAR Image Reconstruction Algorithm Based on 2-D Sparse Decomposition and L_0 Norm Optimization. ***Jour. of GeoSpace Science, 1(1)****, 19-27, 2015*

INTRODUCTION

SAR is an advanced tool for monitoring the relief of the earth's surface by probing with high informative electromagnetic pulses and registration of backscattered radiation (Moreira, 1994), (Nicolas, 2007), (Leijen and Hanssen, 2004) and (Colesanti et al, 2003). The resulting images are depicted in two-dimensional coordinate system defined by the slant range coordinate or coordinate of time delay and azimuth or cross range coordinate. High resolution on the slant range direction is realized by using wide bandwidth emitted pulses while high resolution on the cross range is achieved by coherent summation of reflected signals during the aperture synthesis, the time of observation. Conventional nonparametric SAR imaging algorithms are based on the correlation theory of the matched filter. Their resolution capability is limited by the transmitted signal bandwidth and the synthetic aperture length.

Compressed sensing (CS) is a new approach of sparse signals recovered beyond the Nyquist sampling constraints. It is a high resolution imaging method for SAR sparse targets reconstruction based on CS theory and p norm of Lebesgue vector spaces (Henri Lebesque, 1958). It shows that the image of sparse targets can be reconstructed by solving a convex optimization problem based on l_0 ($p=0$) and/or l_1 ($p=1$) norm minimization with only a small number of SAR echo samples. This indicates the sample size of SAR echo that can be considerably reduced by the CS method. A data acquisition system for wideband SAR imaging and reconstruction of sparse signals from a small set of non-adaptive linear measurements based on CS by exploiting sparseness of point-like targets in the image space and by solving a convex l_1 minimization problem is presented in (Gurbuza et al, 2009).

Corresponding Author: Andon Lazarov, Burgas Free University, 8001, Burgas, 62 San Stefano Street.
E-mail: lazrov@bfu.bg

Instead of measuring sensor returns by sampling at the Nyquist rate, linear projections of the returned signals with random vectors are used as measurements. The applicability of CS method to three dimensional buried point-like targets imaging for continuous-wave ground penetrating radar (SFCW-GPR) is discussed in [6]. It is shown that the image of the sparse targets can be reconstructed by solving a constrained convex optimization problem based on l_1 norm - minimization with only a small number of data from randomly selected frequencies and antenna scan positions, which reduces the data collecting time. Compressive noise radar imaging algorithm that involves the inversion of a linear system characterized by the circulant system matrix generated by the transmit waveform using l_1-based sparsity constraints is analyzed in (Shastryet et al., 2014). The imaging problem is solved using convex optimization.

A data acquisition and imaging method for SFCW-GPRs is presented in (Gurbuz, 2009). It is shown that if the target space is sparse, i.e. a small number of point like targets, it is enough to make measurements at only a small number of random frequencies to construct an image of the target space by solving a convex optimization problem which enforces sparsity through l_1 norm minimization. Based on the assumption that SAR imaging algorithms can reconstruct the target scene with a reduced number of collected samples by applying CS approach authors in (Lin et al., 2010) introduce distributed compressed sensing method into along-track interferometric SAR, achieving good performance for even fewer samples than that based on CS.

A random-frequency SAR imaging scheme based on compressed sensing is proposed in (Yang et al., 2013). It is proven that if the targets are sparse or compressible, it is sufficient to transmit only a small number of random frequencies to reconstruct the image of the targets. A SAR imaging algorithm based on compressed sensing and multiple transmitters multiple azimuth beams is proposed in (Li et al., 2012). This algorithm reconstructs the targets in range and azimuth directions via CS technique, simultaneously provides a high resolution and wide swath two-dimensional map of the spatial distribution of targets with a significant reduction in the number of data samples beyond the Nyquist requirements.

A linear array SAR is a technique to achieve 3-D imaging of earth surface. In this scenario dominating scatterers are always sparse compared with the total 3-D illuminated space cells. Based on a prior knowledge of sparsity property an algorithm for imaging via CS is developed in (Wei et al., 2011). A high resolution imaging method for SAR sparse targets reconstruction based on CS theory is discussed in (Wei et al., 2010). It shows that the image of sparse targets can be reconstructed by solving a convex optimization problem based on l_1 norm minimization with only a small number of SAR echo samples.

Based on the geometrical model of the Earth surface topography and mathematical model of the reflected signals from the relief, and SAR signal's sparse decomposition in the present work a SAR image reconstruction algorithm with application of compressed sensing technique and l_0-norm minimization of the image sparsety is suggested. The rest of the paper is organized as follows. In Section 2 SAR geometry and kinematics are described. In Section 3 a model of SAR signal reflected from the observed surface is derived. In Section 4 a sparse decomposition approach to solve the image reconstruction problem is presented. In Section 5 an image reconstruction algorithm based on sparse decomposition and l_0 norm minimization is discussed. In Section 6 results of a numerical experiment are presented. In Section 7 conclusions are made.

2. SAR geometry and kinematics

Consider SAR geometry and kinematic scenario, defined in coordinate system *Oxyz*. SAR system is located on a spacecraft platform with pre-defined trajectory parameters. The SAR carrier's movement is described by the following vector equation

$$\mathbf{R}(p) = \mathbf{R}_0 + \mathbf{V}T_p\left(\frac{N}{2} - p\right), \tag{1}$$

where $\mathbf{R}_0 = \mathbf{R}(0)$ is the distance vector from the origin of the coordinate system to the satellite at the moment $t = 0$; $\mathbf{V}$ is the satellite velocity vector; T_p is the signal repetition period ; p is the index of emitted pulses; N is the full number of emitted pulses.

The vector equation (1) is projected onto coordinate system *Oxyz*, which yields

$$\begin{aligned} x(p) &= x_0 - V_x T_p\left(\frac{N}{2} - p\right), \\ y(p) &= y_0 - V_y T_p\left(\frac{N}{2} - p\right), \\ z(p) &= z_0 - V_z T_p\left(\frac{N}{2} - p\right), \end{aligned} \tag{2}$$

where $x(p)$, $y(p)$ and $z(p)$ are the satellite coordinates in the moment p; $x_0 = x(0)$, $y_0 = y(0)$ and $z_0 = z(0)$ are the satellite coordinates at the moment $p = 0$; $V_x = V\cos\alpha$, $V_y = V\cos\beta$, $V_z = V\cos\delta$ are coordinates of the velocity vector; $\cos\alpha$, $\cos\beta$, $\cos\gamma$ are the guiding cosines of the velocity vector. The surface of observation is depicted in a coordinate system *Oxyz* and analytically presented as a two dimensional function. The coordinate *z* of this surface is a function of coordinates *x* and *y*, which in discrete form can be expressed as

$$\begin{aligned} z_{mn} &= z_{mn}(x_{mn}, y_{mn}) = 3(1 - x_{mn})^2 \exp[-(x_{mn})^2 - (y_{mn} + 1)^2] \\ &-10\left(\frac{x_{mn}}{5} - x_{mn}^3 - y_{mn}^5\right)\exp\left(x_{mn}^2 - y_{mn}^2\right) \\ &-\frac{1}{3}\exp[-(x_{mn} + 1)^2 - y_{mn}^2] \end{aligned} \tag{3}$$

where $x_{mn} = m\Delta M$ and $y_{mn} = n\Delta N$ are discrete coordinates in the plane *Oxy*; ΔM and ΔN are dimensions of the resolution element in the plane *Oxy*; m and n - relative discrete coordinates (indexes of the resolution element) on axes *Ox* and *Oy*, respectively. Coordinates x_{mn}, y_{mn} and z_{mn} define the distance vector $\mathbf{R}_{mn}$ to each point scatterer from the surface. Assume that in each resolution element with dimensions (ΔM, ΔN) and coordinates (x_{mn}, y_{mn}) one prominent point scatterer is located. During the process of observation the distance vector $\mathbf{R}_{mn}(p)$ from SAR located on the satellite to the dominant point scatterer, defined by the geometrical vector $\mathbf{R}_{mn}$, can be expressed by the following vector equation.

$$\mathbf{R}_{mn}(p) = \mathbf{R}(p) - \mathbf{R}_{mn} \tag{4}$$

The geometrical information of the observed surface is contained in the phase of the complex amplitude of the reflected signal from each point scatterer which is proportional to the module of the distance vector $R_{mn}(p)$ defined by the expression

$$R_{mn}(p)=\sqrt{[x(p)-x_{mn}]^2+[y(p)-y_{mn}]^2+[z(p)-z_{mn}]^2}\ . \qquad (5)$$

The distance $R_{mn}(p)$ is calculated for each p, m and n. In program realization the results of the calculation are placed into three dimensional array with coordinates p, m, and n (Fig. 1).

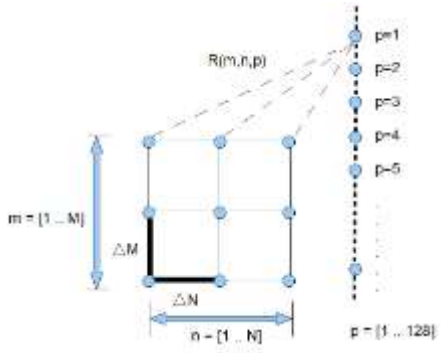

Fig.1: 3-D array of the distances to point scatterers of the surface

3. Modeling of SAR signal reflected from the observed surface

Assume the SAR transmitter emits LFM electromagnetic pulses analytically described by the expression

$$S(t)=\sum_{p=1}^{M}\mathbf{rect}\frac{t-pT_p}{T}\exp\left[-j\left(\omega t+bt^2\right)\right] \qquad (6)$$

where

$$\mathbf{rect}\frac{t-pT_p}{T}=\begin{cases}1, 0\le\dfrac{t-pT_p}{T}<1\\ 0, \text{otherwise}\end{cases}$$

T_p is the pulse repetition period, $\omega=2\pi\dfrac{c}{\lambda}$ is the angular frequency, $p=\overline{1,\ N}$ is the current number of the emitted LFM pulse, N is the total number of emitted pulses during aperture synthesis, $b=\dfrac{\pi\Delta F}{T_k}$ is the LFM index, ΔF is the bandwidth of the emitted pulse, and defines the range resolution, $\Delta R=c/2\Delta F$, $c = 3.10^8$ m/s is the speed of the light, T is the time duration of LFM pulse. The deterministic component of the SAR signal reflected from the *mn*-th point scatterer for particular p as a finite function can be written

$$S_{mn}(t)=a(z_{mn}).\mathbf{rect}\frac{t-t_{mn}}{T}.\exp\left\{-j\left[\omega(t-t_{mn})+b(t-t_{mn})^2\right]\right\} \qquad (7)$$

where

$$\mathbf{rect}\frac{t-t_{mn}(p)}{T_k}=\begin{cases}1, \dfrac{t-t_{mn}(p)}{T_k}\le 1,\\ 0, \text{otherwise}\end{cases} \qquad (8)$$

$a(z_{mn})$ is the reflectivity coefficient of the *mn*-th point scatterer, $t_{mn}(p)=\dfrac{2R_{mn}(p)}{c}$ is the time delay of the signal from the *mn*-th point scatterer. The deterministic component of the SAR signal reflected from the entire surface can be regarded as a geometrical sum of the signals reflected by all point scatterers from the surface of observation and can be expressed as

$$S(t)=\sum_{n}\sum_{m}a(z_{mn}).\mathbf{rect}\frac{t-t_{mn}(p)}{T_k}.\exp\left\{-j\left[\omega\left(t-t_{mn}(p)\right)+b(t-t_{mn}(p))^2\right]\right\}, \quad (9)$$

where $t=t_{mn\min}(p)+(k-1)\Delta T$ is the fast time in discrete form for each p, measured on the range direction, $k=\overline{0,K_{\max}(p)-1}$ is the range sample (fast time) index, ΔT is the timewidth of the LFM sample, $K_{\max}(p)$ is the number of the range bin where the SAR signal from the furthest point scatterer is detected, $t_{mn\min}(p)=\frac{2R_{mn\min}(p)}{c}$ is the time delay of the signal from the nearest point scatteter, $R_{mn\min}(p)$ is the distance to the nearest point scatteter on the surface of observation, calculated for the p-th emitted pulse.

Based on Taylor expansion of the exponential power, $\omega\left(t-t_{mn}(p)\right)+b(t-t_{mn}(p))^2$ in the vicinity of unknown discrete coordinates $\hat{p}$ and $\hat{k}$ of the mn-th point scatterers, (9) can be rewritten as

$$S(p,k)=\sum_{\hat{p},\hat{k}}a(\hat{p},\hat{k}).\mathbf{exp}\left\{-j\left[2.\pi.\frac{p.\hat{p}}{\hat{N}}+2.\pi.\frac{k.\hat{k}}{\hat{K}}+\Phi(p,k)\right]\right\}, \quad (10)$$

where $a(\hat{p},\hat{k})$ is the image function - the projection of $a(z_{mn})$ onto (p, k) signal plane, $\Phi(p,k)$ is the phase term of second and higher order, $\hat{p}=\overline{0,\hat{N}-1}$, $\hat{k}=\overline{0,\hat{K}-1}$, $\hat{N}$ and $\hat{K}$ denote the full number of reference image points on cross range direction and range direction, respectively.

4. Sparse decomposition approach to solve the image reconstruction problem

Assume $\Phi(p,k)=0$, then (10) in matrix form can be rewritten as (Qui et al., 2013)

$$\mathbf{S}=\mathbf{P}.\mathbf{A}.\mathbf{K}^T \quad (11)$$

where $\mathbf{S}_{(N\times K)}$ is the full length signal matrix, $\mathbf{P}_{(N\times\hat{N})}=\left[\exp\left(-j\frac{2\pi p.\hat{p}}{\hat{N}}\right)\right]$ is the cross range discrete Fourier transform (DFT) matrix, cross-range matrix-dictionary, $\mathbf{K}_{(K\times\hat{K})}=\left[\exp\left(-j\frac{2\pi k.\hat{k}}{\hat{K}}\right)\right]$ is the range DFT matrix, range matrix-dictionary, $\mathbf{A}_{(\hat{N}\times\hat{K})}$ is the image matrix. Expression (11) denotes 2-D discrete Fourier decomposition of the SAR signal in matrix form. It means that the two-dimensional signal $\mathbf{S}\in\mathbf{R}^{N\times K}$ is a linear combination of columns of matrices $\mathbf{P}$ and $\mathbf{K}$. In case $N=\hat{N}$ (complete measurement) the decomposition (11) is unique, it means that there exists a unique sparsest solution for $\mathbf{A}$. Define a compressed measurement matrix

$$\mathbf{X}=\mathbf{\Phi}_p.\mathbf{S}.\mathbf{\Phi}_k^T+\mathbf{W}\in\mathbf{R}^{N'\times K'}, \quad (12)$$

over the redundant Fourier dictionaries $\hat{\mathbf{P}}=\mathbf{\Phi}_p.\mathbf{P}\in\mathbf{R}^{N'\times\hat{N}}$ and $\hat{\mathbf{K}}=\mathbf{\Phi}_k\mathbf{K}\in\mathbf{R}^{K'\times\hat{K}}$, where $\mathbf{\Phi}_{p(N'\times N)}$ and $\mathbf{\Phi}_{k(K'\times K)}$ are pseudo identity sensing matrices, $\mathbf{W}$ is the white Gaussian noise matrix. In overcomplete case $N'<\hat{N}$ and $K'<\hat{K}$ the matrix $\mathbf{X}$ does not have unique decomposition. The image reconstruction problem can be solved by definition of sparse decomposition of the measurement signal as follows

$$\mathbf{min}\|\mathbf{A}\|_0 \text{ subject to } \left\|\mathbf{X}-\hat{\mathbf{P}}.\mathbf{A}.\hat{\mathbf{K}}^T\right\|_2^2\le\varepsilon, \quad (13)$$

image matrix $\mathbf{A}$, that means to find out the image matrix $\mathbf{A}$ with as much zero entries as possible, $\left\|\mathbf{X}-\hat{\mathbf{P}}.\mathbf{A}.\hat{\mathbf{K}}^T\right\|_2^2$ denotes the square of the Euclidian norm, ε is a small constant. A Gaussian function is used to approximate the l_0 - norm, i.e.

$$\|\mathbf{A}\|_0 = \hat{N}.\hat{K} - \sum_{\hat{p}=0}^{\hat{N}-1}\sum_{\hat{k}=0}^{\hat{K}-1}\exp\left(-\frac{\hat{a}_{\hat{p},\hat{k}}^2}{2\sigma^2}\right) \tag{14}$$

where σ is the variance of the white Gaussian noise. Then l_0-norm, $\min\|\mathbf{A}\|_0$ can be obtained be maximizing of the Gaussian function $F_\sigma(\mathbf{A}) = \sum_{\hat{p}=0}^{\hat{N}-1}\sum_{\hat{k}=0}^{\hat{K}-1}\exp\left(-\frac{\hat{a}_{\hat{p},\hat{k}}^2}{2\sigma^2}\right)$ onto the feasible set $\left\{\mathbf{A}\middle|\mathbf{X}=\hat{\mathbf{P}}.\mathbf{A}.\hat{\mathbf{K}}^T\right\}$ by a steepest ascent algorithm followed by projection onto the feasible set. Maximization of $F_\sigma(\mathbf{A})$ means increasing the number of zeros entries in the image matrix $\mathbf{A}$.

5. Image reconstruction algorithm based on sparse decomposition and l_0 norm minimization

The modified image reconstruction algorithm (Ghaffari et al., 2009) and (Mohimani et al., 2009):

1. Calculate initial estimate of the image matrix $\hat{\mathbf{A}}_0$, using Euclidian norm $\left\|\mathbf{X}-\hat{\mathbf{P}}.\mathbf{A}.\hat{\mathbf{K}}^T\right\|_2^2=0$, which corresponds to an initial variance $\sigma_0=\infty$, i.e.

$$\hat{\mathbf{A}}_0 = \hat{\mathbf{P}}^*.\mathbf{X}.(\hat{\mathbf{K}}^*)^T, \tag{15}$$

where $\hat{\mathbf{P}}^* = \left[\exp\left(j\frac{2\pi p.\hat{p}}{\hat{N}}\right)\right]$, $\hat{\mathbf{K}}^* = \left[\exp\left(j\frac{2\pi k.\hat{k}}{\hat{K}}\right)\right]$ are the cross range inverse DFT matrix and range inverse DFT matrix, respectively.

2. Define the next value of the variance $\sigma_1 = (2-4).(\max\left|\hat{a}_{\hat{p},\hat{k}}\right|)$ where $(\max\left|\hat{a}_{\hat{p},\hat{k}}\right|)$ is the maximum absolute value of the entry in the matrix $\hat{\mathbf{A}}_0$.

3. Define decreasing sequence of variances $\sigma_j = c.\sigma_{j-1}$, where $j=\overline{2,J}$, $0.5\le c\le 1$, and for each σ_{j-1}, calculate the $F_\sigma(\mathbf{A}) = \sum_{\hat{p}=0}^{\hat{N}-1}\sum_{\hat{k}=0}^{\hat{K}-1}\exp\left(-\frac{\hat{a}_{\hat{p},\hat{k}}^2}{2\sigma_{j-1}^2}\right)$ and $\|\mathbf{A}\|_0$ by expression (15) .

Steepest ascending algorithm for SAR imaging

4. Initialization: Let $\mathbf{A}=\hat{\mathbf{A}}_{j-1}$, obtained for $\sigma=\sigma_{j-2}$. Define the decreasing matrix $\mathbf{\Delta}=[\delta_{\hat{p},\hat{k}}]=[-\sigma_{j-2}^2.(\nabla F_{\sigma\,j-2})]$, where ∇ is the nabla operator over $F_{\sigma\,j-2}$, then $\delta_{\hat{p},\hat{k}} = \hat{a}_{\hat{p}.\hat{k}}.\exp\left(-\frac{\hat{a}_{\hat{p},\hat{k}}^2}{2\sigma_{j-2}^2}\right)$.

5. Calculate $\hat{\mathbf{A}}_j = \hat{\mathbf{A}}_{j-1} - \Delta$. If $\hat{\mathbf{A}}_j < \hat{\mathbf{A}}_{j-1}$, go to step 3. In case the matrix $\hat{\mathbf{A}}_j$ does not change, then project matrix $\hat{\mathbf{A}}_{j-1}$ back onto the feasible set $\left\{\mathbf{A}\middle|\mathbf{X} = \hat{\mathbf{P}}.\mathbf{A}.\hat{\mathbf{K}}^T\right\}$, i.e. $\mathbf{A}_j = \mathbf{A}_{j-1} - \hat{\mathbf{P}}^*(\hat{\mathbf{P}}.\mathbf{A}_{j-1}.\hat{\mathbf{K}}^T - \mathbf{X})(\hat{\mathbf{K}}^*)^T$.

6. The procedure is repeated until $\mathbf{A}_j = \mathbf{A}_{j-1}$ or $\|\mathbf{A}\|_0$ does not decrease anymore. In practice, the termination of the optimization procedure can be performed when $\|\mathbf{A}_{j-1}\|_0 - \|\mathbf{A}_j\|_0 \leq 10^{-2}$.

6. Numerical experiment

Consider SAR scenario defined by the following parameters. Initial coordinates of the SAR carrier: $x_0 = 10^4$ m, $y_0 = 10^4$ m, $z_0 = 8.10^5$ m, vector velocity: $V = 10^3$ m/s, guiding angles: $\alpha = \pi\backslash 4$, $\beta = \pi\backslash 4$, $\gamma = 0$. SAR parameters: carrier frequency 10^{10} Hz, frequency bandwidth $\Delta F = 2{,}5.10^7$ Hz, pulse repetition period $2{,}5.10^{-3}$ s, LFM pulse width $2{,}5.10^{-6}$ s, number of emitted pulses $N_p = 1024$, number of range samples $K = 1024$. The geometry of the observed scene is defined by standard "peaks" function. The original image of the relief with dimensions [1024×1024] pixels described by the function "peaks" is depicted in Fig. 2.

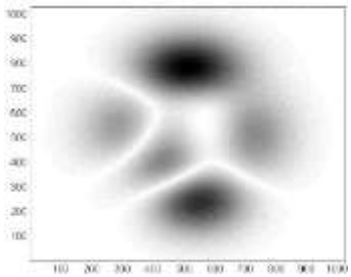

Fig. 2: Original image of the observed surface

The full length SAR signal reflected from the "peaks" surface, modeled by the matrix decomposition (11) of the signal matrix $\mathbf{S}(1024\times1024)$ is presented in Fig. 3.

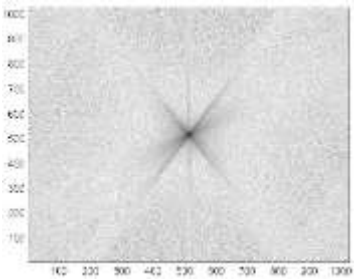

Fig. 3: Full length SAR signal modeled by decomposition (11)

Compressed sensing measurement matrix $\mathbf{X}(64\times64)$ obtained by the multiplication of the signal complex matrix $\mathbf{S}(1024\times1024)$ with sensing pseudo identity matrices $\mathbf{\Phi}_{p(64\times1024)}$ and $\mathbf{\Phi}_{k(64\times1024)}$, and additive Gaussian noise $\mathbf{W}(64\times64)$ (Eq. 12), is presented in Fig. 5. As can be seen in Fig. 5 the final image obtained from compressed sensing measurement data and reconstructed by application of l_0 norm optimization has satisfactory resolution.

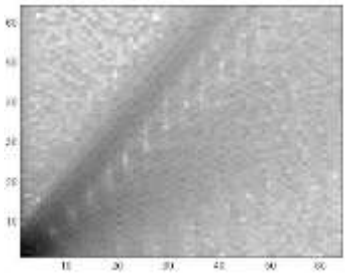

Fig. 4: SAR signal after application of compressed sensing approach to full length data

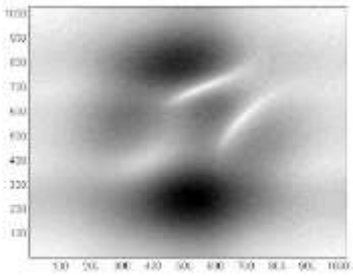

Fig. 5: Final image obtained from compressed sensing measurement data and reconstructed by application of l_0 norm optimization

In comparison with the original image of the observed surface (Fig. 2), the main peaks of the observed surface are clearly defined in the image obtained by compressed sensing of measurement data (Fig. 5). The computational results prove the correctness of the signal mathematical model and image reconstruction algorithm based on sparse decomposition of the SAR signal and l_0 norm minimization.

Conclusion

A SAR image reconstruction algorithm based sparse decomposition has been developed. A model of LFM SAR signal reflected from the observed scene - the relief of the earth surface, has been presented as a matrix multiplication of three matrices: azimuth (cross range) inverse discrete Fourier transform (IDFT) matrix, image matrix and range IDFT matrix. Image reconstruction procedure based on l_0 norm optimization has been developed and applied over reduced number of measurements defined by randomly generated azimuth and range sensing matrices. The geometry of the scene has been described by standard “peaks” function. Results of numerical experiments have been provided to prove correctness of the developed algorithm.

References

[1] Moreira A., 1994, Airborne SAR Processing of Highly Squinted Data Using a Chirp Scaling Algorithm with Motion Compensation. IEEE Trans. on GRS, 32(5), 1029-1040.

[2] Nicolas J-M, Vasile G., 2007, Gay, M.; Tupin, Fl.; Trouvé, Em.: SAR processing in the temporal domain: application to direct interferogram generation and mountain glacier monitoring Can. J. Remote Sensing, Vol. 33, No. 1, 52–59.

[3] Leijen V., Hanssen F. R., 2004, Interferometric radar meteorology: resolving the acquisition ambiguity. In CEOS SAR Workshop, Ulm Germany, 27-28, 6-14.

[4] Colesanti C., Ferretti Al., 2003, Novali, F.; Prati, Cl.; Rocca, F.: SAR monitoring of progressive and seasonal ground deformation using the Permanent Scatterers Technique. IEEE Transactions on Geoscience and Remote Sensing, 41(7), 1685-1701.

[5] Gurbuza A.C., McClellanb, J.H., Waymond R., Scott Jr. b., 2009, Compressive sensing for subsurface imaging using ground penetrating radar, Signal Processing, 89 (10), 1959–1972.
[6] Cai J. L., Tong C. M., Zhong W. J., Ji W. J., 2012, 3D imaging method for stepped frequency ground penetrating radar based on compressive sensing, Progress in Electromagnetics Research M, 23, 153-165.
[7] Shastry M.C., Narayanan R.M., Rangaswamy M., 2014, Analysis of the tolerance of compressive noise radar systems to multiplicative perturbations. Proc. SPIE 9109, Compressive Sensing III, 910905.
[8] Gurbuz A. C., McClellan J. H., Scott W. R., 2009, A compressive sensing data acquisition and imaging method for stepped-frequency GPRs. IEEE Transaction on Signal Processing, Vol. 57, No. 7, 2640-2650.
[9] Lin Y.G., Zhang B.C., Hong W., Wu Y.R., 2010, Along-track interferometric SAR imaging based on distributed compressed sensing. Electronics Letters, 46 (12), 858 – 860.
[10] Yang J., Thompson J., Huang X., Jin T., 2013, Random-Frequency SAR Imaging Based on Compressed Sensing, Geoscience and Remote Sensing. IEEE Transactions on, 51 (2), 983 – 994.
[11] Li J., Zhang S., Chang J., 2012, Applications of compressed sensing for multiple transmitters multiple azimuth beams SAR imaging. Progress in Electromagnetics Research, 127, 259-275.
[12] Wei S. J., Zhang X. L., Shi J., 2011, Linear array SAR imaging via compressed sensing. Progress In Electromagnetics Research, 117, 299-319.
[13] Wei S. J., Zhang X. L., Shi J., Xiang G., 2010, Sparse reconstruction for SAR imaging based on compressed sensing. Progress in Electromagnetics Research, 109, 63-81.
[14] Qiu W., Giusti E., Bacci A., Martorella M., Berizzi F. et al., 2013, Compressive sensing for passive ISAR with DVB-T signal. In Proceedings of IRS-2013, 113-118 19-21.
[15] Ghaffari A., Zadeh B. M., Jutter C., Moghaddam H., 2009, Sparse decomposition of two-dimensional signals. Proceedings of IEEE International Conference on Acoustics, Speech and Signal Processing, 3157-3160.
[16] Mohimani H., Babaie-Zadeh B. M., Jutten C., 2009, A fast approach for overcomplete sparse decomposition based on smoothed norm. IEEE Trans. on Signal Proc, 57 (1), 289–301.